Journal of Catalysis **189,** 79–90 (2000)
Article ID jcat.1999.2703, available online at http://www.idealibrary.com on IDEAL®

Probing the Basic Character of Alkali-Modified Zeolites by CO_2 Adsorption Microcalorimetry, Butene Isomerization, and Toluene Alkylation with Ethylene

Shailendra V. Bordawekar and Robert J. Davis[1]

Department of Chemical Engineering, University of Virginia, Charlottesville, Virginia 22903-2442

Received May 26, 1999; revised September 22, 1999; accepted September 27, 1999

Two types of alkali-modified zeolites *X* and *Y* were studied, namely, zeolites containing occluded cesium oxides and zeolites containing occluded alkali metals (Na, Cs). Zeolites with occluded CsO_X, obtained via impregnation and decomposition of cesium acetate, exhibited higher CO_2 adsorption capacities and higher heats of adsorption than the corresponding ion-exchanged zeolites. However, the heats of adsorption were significantly lower on the zeolite-supported oxides (∼85 kJ mol^{-1}) compared to bulk cesium oxide (∼270 kJ mol^{-1}). The CO_2 adsorption capacities of the zeolites containing occluded CsO_X increased linearly with the amount of occluded cesium (1 CO_2 per 4 occluded Cs atoms), and the catalytic activity for 1-butene isomerization was commensurate with the CO_2 uptake on the materials. Stronger base sites were created in zeolites by decomposition of impregnated alkali azides (Na, Cs), due to the formation of alkali metal species. These materials were active catalysts for the side-chain alkylation of toluene with ethylene, whereas zeolites containing occluded CsO_X were inactive for the reaction. Dioxygen adsorption followed by thermal treatment of zeolites containing occluded alkali metal resulted in the elimination of their activity for toluene alkylation whereas their activity for butene isomerization was retained. Alkali oxide- and alkali metal-containing microporous carbon materials exhibited significantly different adsorption properties and catalytic activities from their zeolite counterparts, possibly due to the different nature of the occluded species and/or steric constraints in the amorphous carbon.

© 2000 Academic Press

INTRODUCTION

Zeolites containing exchanged alkali cations are basic materials that catalyze many reactions, including double-bond isomerization of olefins, side-chain alkylation of aromatics with methanol, dehydrogenation of alcohols, and Knoevenagel condensation of aldehydes (1–5). The base sites in ion-exchanged zeolites are the framework oxygen atoms (2). The base strength and catalytic activity of alkali-exchanged zeolites can be increased significantly by occlusion of alkali oxide clusters via impregnation and decomposition of alkali compounds (1–3, 6–9). Highly basic zeolites can also be obtained by incorporation of alkali metal clusters in the zeolite supercages. These clusters are thought to enhance the basicity by increasing the negative charge on the framework oxygen atoms of the zeolite (2). However, the metal itself may also be an active site. The synthesis and characterization of metallic and ionic alkali clusters in zeolites has been described previously (10–15). For example, incorporating sodium metal into nonacidic zeolites can be accomplished by vapor deposition of hot bulk metal (10), impregnation with a solution of sodium metal in liquid ammonia (16), and thermal decomposition of impregnated sodium azide (11, 17). Martens *et al.* detected three different kinds of Na species in these materials by ESR spectroscopy, namely, an extralattice metal phase, intracrystalline neutral Na clusters, and ionic Na clusters (11). A comparison of the ESR spectra of sodium metal-containing zeolites prepared by each of the three methods mentioned above showed that the thermal decomposition of impregnated alkali azide resulted in an abundance of intracrystalline neutral sodium clusters which were also catalytically the most active species (12). Apparently, decomposition of impregnated azide is an efficient method for obtaining highly basic alkali metal/zeolite catalysts.

Even though basic zeolites have been investigated as catalysts, very little is known about the nature of their basic sites. In this work, we studied zeolites containing occluded alkali metals and alkali metal oxides. Alkali metals and oxides were also supported on a nonoxidic carrier, microporous carbon, to compare the effect of support composition on basicity. The base sites in these materials were characterized by adsorption microcalorimetry of carbon dioxide to determine both the enthalpy of formation and the stoichiometry of the adsorbed complex. To correlate characterization results with catalytic function, the activity of these basic materials was examined for the double-bond isomerization of 1-butene and the side-chain alkylation of toluene with ethylene. These reactions are interesting because differences in product selectivities depend on whether the catalyst is acidic or basic. For butene isomerization, acidic

[1] To whom correspondence should be addressed.

0021-9517/00 $35.00
Copyright © 2000 by Academic Press
All rights of reproduction in any form reserved.

catalysts yield product 2-butenes having a *cis*/*trans* ratio near unity, whereas basic catalysts yield predominantly the *cis* product. For toluene alkylation, an acid-catalyzed reaction results in alkylation of the aromatic ring, whereas a base-catalyzed reaction leads to selective alkylation of the side chain (2).

EXPERIMENTAL

Catalyst Synthesis

Cesium-exchanged *X* and *Y* zeolites were prepared by triply ion-exchanging Na*X* (Union Carbide, lot no. 943191060078) and Na*Y* (Union Carbide, lot no. 955089001010-S) with 1 M aqueous solution of cesium acetate (Aldrich 99.9%). The zeolite was slurried in the aqueous solution for 2 h during each exchange and then vacuum-filtered. Each sample was subsequently washed with distilled, deionized water. The resultant ion-exchanged materials were dried overnight in air at 373 K and calcined in flowing air at 773 K for 5 h. The heating rate during calcination was 4 K min^{-1} to avoid collapse of the zeolite framework due to steaming.

Samples containing excess alkali species (in addition to the ion-exchanged cations) were prepared by impregnation of the ion-exchanged zeolites with solutions of alkali compounds. Two different types of occluded species, namely, alkali oxide clusters and alkali metal clusters, were obtained by using the appropriate alkali precursor and decomposition procedure, as described below.

Zeolites containing occluded oxide clusters are referred to as CsO_X/Cs*X* and CsO_X/Cs*Y*. These were obtained by incipient wetness impregnation of the cesium-exchanged zeolites with aqueous solutions of cesium acetate of the appropriate concentration. The impregnated catalysts were dried overnight in air at 373 K and calcined in flowing air at 773 K for 5 h.

Zeolites containing occluded alkali metal clusters are referred to as alkali/alkali-*X* and alkali/alkali-*Y*, where "alkali" stands for Na or Cs. These catalysts were synthesized using alkali azide precursors. The ion-exchanged zeolites were stirred in a solution of alkali azide (NaN_3 99% or CsN_3 80–90 wt% in methanol, Acros) in excess methanol at room temperature until the methanol evaporated. The samples were dried overnight in air at 373 K. These catalysts were pretreated *in situ* before adsorption or catalytic experiments to decompose the azide and obtain the supported alkali metal. During pretreatment, the catalysts were heated to 523 K at 4 K min^{-1} and held at this temperature for 1 h to desorb zeolitic water. The temperature was then ramped at 1 K min^{-1} to the final temperature (673 K for NaN_3 and 873 K for CsN_3) and held at this temperature for 5 h. The presence of alkali metals in zeolites, after decomposition of the impregnated alkali azides, was confirmed by ESR spectroscopy (18).

In addition to alkali-modified zeolite catalysts, alkali-modified microporous carbon catalysts were also studied in this work. Microporous carbon (Armak, lot no. 50901) was impregnated with an aqueous solution of cesium acetate of the appropriate concentration, to the point of incipient wetness. The sample was dried overnight in air at 373 K and pretreated in flowing He at 773 K for 5 h. This sample is labeled CsO_X/C. Alkali azide-modified carbon was synthesized by impregnating the carbon with a solution of NaN_3 in excess methanol, using a procedure similar to that used for alkali azide-modified zeolites discussed earlier. Postsynthesis treatment of this sample (Na/C) was also similar to that used for sodium azide-modified zeolites.

Elemental analyses of the alkali ion-exchanged zeolites were performed by Galbraith Laboratories, Inc., Knoxville, TN.

Catalyst Characterization

The presence of heavy alkali metals in the zeolite pores attenuates the X-ray diffraction peak intensities. Thus, physical adsorption was used to verify the structural integrity of the zeolite samples. The BET surface areas and pore volumes of the catalysts were obtained from dinitrogen adsorption isotherms measured at 77 K on a Coulter Omnisorp 100CX instrument after the catalysts outgassed for 10–12 h at 573 K. Pore volumes were determined from the liquid volume of dinitrogen adsorbed at a relative pressure of 0.3.

The energetics of the adsorption sites of alkali-modified zeolites were obtained via microcalorimetry of carbon dioxide adsorption, and in some cases dioxygen adsorption. The microcalorimeter apparatus used in these experiments is described elsewhere (19). The alkali-exchanged and CsO_X-occluded zeolites were pretreated at 773 K for 5 h under vacuum, prior to carbon dioxide adsorption. The alkali azides loaded into zeolites were decomposed *in situ* for 5 h under vacuum. The pretreatment temperatures were 673 K for NaN_3 and 873 K for CsN_3. All of the adsorption experiments were conducted isothermally at 373 K.

X-ray photoelectron spectroscopy was used to obtain the relative alkali compositions on the surfaces of alkali-modified zeolites. The XPS spectra were collected on a PHI 560 ESCA/SAM system (Perkin-Elmer) operated in the constant pass energy (50 eV), with a Mg*Kα* anode. Although the sample powder was spread on a conductive carbon tape, sample charging was also minimized by using an electron-flood gun. The spectra were recorded for Cs $3d_{5/2}$, Na 1*s*, and Si 2*s* core lines.

Catalytic Reactions

The double-bond isomerization of 1-butene was carried out in a single-pass quartz fixed-bed reactor at 373 K and atmospheric pressure. The catalysts were pretreated in

flowing He using the same pretreatment procedures for adsorption microcalorimetry. The reactant stream consisted of He (BOC gases) and 1-butene (Aldrich, 99+%) in a molar ratio of 9 : 1. The total flow rate of the reactant stream was 10 ml min^{-1} at STP. Reaction products were analyzed using an on-line gas chromatograph (Hewlett–Packard 5890 Series II) equipped with a 50-m HP-PLOT/Al_2O_3 capillary column. The typical conversions of 1-butene in these experiments were less than 20%.

The alkylation of toluene with ethylene was carried out in a single-pass quartz fixed-bed reactor at 523 K and atmospheric pressure. The azide samples were decomposed in flowing He prior to the reaction, using the pretreatment procedures discussed earlier. Liquid toluene was pumped at a rate of 0.5 ml min^{-1} and vaporized into a flowing stream of He and ethylene. The molar ratios of He to ethylene to toluene in the reactant stream were 16 : 10 : 1. Reaction products were analyzed using an on-line gas chromatograph (Hewlett–Packard 5890 Series II) equipped with a 50-m HP-1 capillary column.

RESULTS AND DISCUSSION

Results from Elemental Analysis and Physical Adsorption

The unit cell compositions of the Na forms of the *X* and *Y* zeolites, obtained from elemental analyses, are reported in Table 1. These are expressed in terms of an ideal faujasite unit cell having 384 oxygen atoms bridging Si and Al tetrahedra.

The properties of zeolite *X* containing occluded CsO_X clusters are summarized in Table 2. Results from a similar set of *Y* zeolites were similar to those presented in Table 2. Occlusion of CsO_X clusters resulted in a moderate decrease in the surface area of the zeolites. There was also a decrease in the specific pore volume with increasing amounts of occluded CsO_X. Similarly, zeolites containing occluded alkali metals showed a decrease in surface areas and pore volumes (Table 3) compared to their ion-exchanged counterparts. The pore volumes for zeolites containing occluded alkali species reported in Tables 2 and 3 are expressed per gram of the loaded zeolite. However, the corrected pore volumes calculated per gram of the corresponding ion-exchanged zeolites were not significantly different (<10%) from the values reported in the tables.

TABLE 1

Compositions and BET Surface Areas of Alkali-Exchanged Zeolites

Zeolite	Unit cell composition	BET surface area ($m^2\ g^{-1}$)
Na*X*	$Na_{78.8}Si_{104.3}Al_{87.7}O_{384}$	766
Na*Y*	$Na_{53.7}Si_{138}Al_{54.1}O_{384}$	863

TABLE 2

Compositions, BET Surface Areas, and Pore Volumes of CsO_X/Cs*X* Zeolites

Zeolite[a]	Unit cell composition	No. of occluded Cs atoms per unit cell	BET surface area ($m^2\ g^{-1}$)	Pore volume (ml g^{-1})
Cs*X*(1)	$Cs_{41.4}Na_{32.5}Si_{106.7}Al_{85.3}O_{384}$	0.0	503	0.204
CsO_X/Cs*X*(1)	—	1.3	439	0.184
Cs*X*(2)	$Cs_{40.0}Na_{32.5}Si_{106.1}Al_{85.9}O_{384}$	0.0	495	0.203
CsO_X/Cs*X*(2)	—	4.0	396	0.165
Cs*X*(3)	$Cs_{52.6}Na_{33.3}Si_{105.8}Al_{86.2}O_{384}$	0.0	453	0.189
CsO_X/Cs*X*(3)	—	6.7	374	0.157
Cs*X*(4)	$Cs_{40.2}Na_{34.2}Si_{106.6}Al_{85.4}O_{384}$	0.0	452	0.189
CsO_X/Cs*X*(4)	—	10.7	336	0.141
Cs*X*(5)	$Cs_{38.6}Na_{38.3}Si_{106.8}Al_{85.2}O_{384}$	0.0	495	0.200
CsO_X/Cs*X*(5)	—	16.0	324	0.133
Cs*X*(6)	$Cs_{50.9}Na_{35.6}Si_{106.5}Al_{85.5}O_{384}$	0.0	501	0.201
CsO_X/Cs*X*(6)	—	21.3	214	0.088

[a] Each CsO_X/Cs*X* sample was prepared using the corresponding Cs*X* sample.

Analogous properties of alkali-modified carbon catalysts, summarized in Table 4, also indicate a decrease in surface areas and pore volumes compared to the bare carbon support.

Microcalorimetry of CO_2 Adsorption on CsO_X/CsX and Bulk "Cs_2O"

Differential heats of adsorption as a function of CO_2 uptake for CsO_X/Cs*X* zeolites with different loadings of occluded cesium are shown in Fig. 1. In each of these samples, there were a few sites with high heats of CO_2 adsorption (>100 kJ mol^{-1}). The adsorption energies decreased rapidly to a plateau, indicating that a majority of the sites had uniform strength. The thermogram for Cs*X* without occluded alkali is also included in Fig. 1, for comparison. Incorporation of occluded CsO_X in Cs*X* increased the total number of base sites as well as their strength. Even though the number of base sites increased with increasing amounts of

TABLE 3

Properties of Zeolites Containing Occluded Alkali Metals

Zeolite	No. of occluded alkali atoms per unit cell	BET surface area ($m^2\ g^{-1}$)	Pore volume (ml g^{-1})
Na/Na*X*	51	201	0.083
Cs/Na*X*	8	554	0.222
Na/Cs*X*	67	141	0.063
Cs/Cs*X*	20	163	0.072
Cs/Na*Y*	14	496	0.200

TABLE 4

Properties of Alkali-Modified Carbon Catalysts

Sample	wt% alkali[a]	BET surface area ($m^2\ g^{-1}$)	Pore volume ($ml\ g^{-1}$)
Carbon	0.0	843	0.409
CsO_X/C	16.0	728	0.299
Na/C	8.9	694	0.286

[a] Based on weight of bare support.

occluded CsO_X, the strengths of a majority of the sites in CsO_X/Cs*X* seemed to be unaffected by the CsO_X loading. Most of the adsorption sites in each of the CsO_X/Cs*X* samples have energies close to 85 kJ mol^{-1}. Results from CO_2 adsorption microcalorimetry on CsO_X/Cs*Y* zeolites were similar to those for CsO_X/Cs*X*.

It is believed that the decomposition of cesium acetate occluded in cesium-exchanged zeolites leads to the formation of cesium oxide clusters (1, 6, 20, 21). These occluded moieties are apparently more basic than the framework oxygen atoms of the zeolite. Lasperas *et al.* studied a series of Cs*X* and Cs*Y* zeolites with different loadings of occluded Cs by TPD of adsorbed CO_2 (6). They observed the amount of CO_2 desorbed (up to 773 K) was proportional to the amount of excess cesium, up to 16 Cs atoms per unit cell of Cs*X*. Since the stoichiometry was measured to be about one CO_2 molecule desorbed for every two added Cs atoms, Lasperas *et al.* concluded that the composition of the occluded species was Cs_2O.

Figure 2 shows the total CO_2 uptake obtained from adsorption microcalorimetry as a function of the number of occluded Cs atoms in CsO_X/Cs*X* and CsO_X/Cs*Y*. The CO_2 adsorption capacity of these zeolites increased linearly with

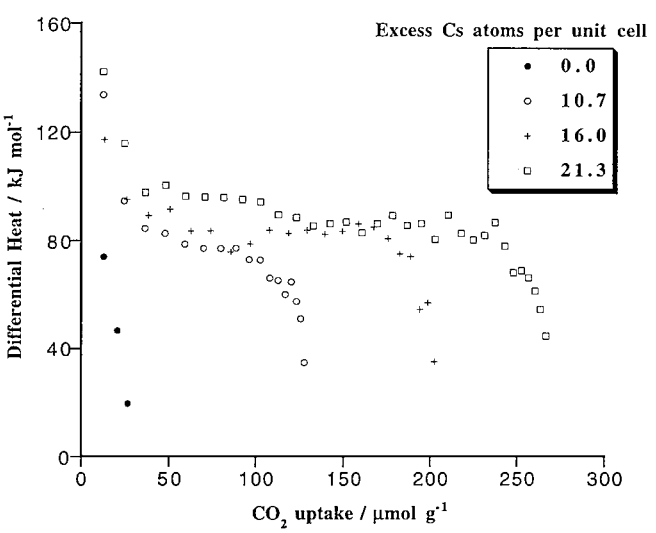

FIG. 1. Differential heats of adsorption as a function of CO_2 uptake for CsO_X/Cs*X* zeolites.

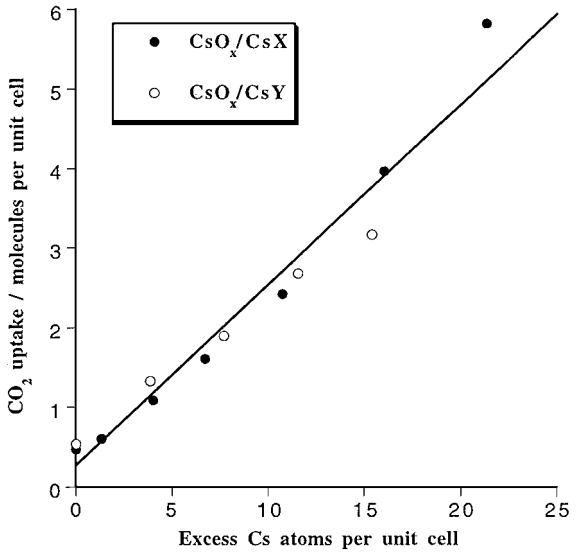

FIG. 2. Carbon dioxide adsorption capacity of zeolites containing occluded CsO_X as a function of the number of occluded Cs atoms.

the amount of occluded Cs. This result is consistent with the observation of Lasperas *et al.* (6). However, in our case, about one CO_2 molecule was adsorbed for every four occluded Cs atoms, which does not support the ideal formula of Cs_2O for the occluded cesium oxide.

As a reference for the cesium oxides occluded in zeolites, the enthalpy of CO_2 adsorption was measured at 373 K on bulk "Cs_2O" (Aldrich 99+%) pretreated at 623 K for 5 h under vacuum. The strongest sites on the bulk oxide had ΔH_{ads} of about 270 kJ mol^{-1}. Thus, the bulk oxide had significantly stronger sites than those in CsO_X/Cs*X* and CsO_X/Cs*Y*. However, the commercial bulk "Cs_2O" sample was probably not a pure compound, but may have contained a mixture of cesium suboxides, peroxides, and superoxides with an average formula claimed to be Cs_2O. Krawietz *et al.* performed MAS NMR studies on various oxides of cesium and found that commercial bulk "Cs_2O" samples were mixtures of Cs_2O_2 and CsO_2 (22). The heat of reaction for $\{Cs_2O + CO_2 \rightarrow Cs_2CO_3\}$ obtained from the heats of formation data for the constituent compounds was −402 kJ mol^{-1} (23). This value is significantly greater than the heat of CO_2 adsorption measured on our bulk "Cs_2O" (270 kJ mol^{-1}). Nevertheless, the difference in the adsorption energies of CsO_X clusters occluded in zeolites and the bulk "Cs_2O" compound from Aldrich indicates that the zeolite-occluded cesium species had a very different character than the bulk oxide.

Decomposition of cesium compounds at high temperatures can lead to the formation of various cesium oxides, depending on the gaseous environment. It is possible to synthesize cesium superoxide (CsO_2), cesium peroxide (Cs_2O_2), cesium oxide (Cs_2O), and cesium suboxide (Cs_7O) by varying the dioxygen concentration. Kim *et al.* studied

the loss of oxygen from bulk "Cs_2O" heated to various temperatures and proposed that it decomposed to Cs_7O, at least on the surface, at temperatures above 623 K in an inert atmosphere (7). Kim *et al.* also observed a higher *cis*/*trans* ratio of the product 2-butenes in the isomerization of 1-butene for "Cs_2O" pretreated at 423 K compared to "Cs_2O" pretreated at 623 K (7).

To test the effect of pretreatment temperature on the heat of CO_2 adsorption for bulk "Cs_2O", microcalorimetry experiments were carried out on bulk oxide samples pretreated at 423 and 773 K for 5 h under vacuum. The initial heats of CO_2 adsorption for the different pretreatment temperatures were within 10% of each other, indicating that the pretreatment temperature did not have a significant effect. However, bulk "Cs_2O" pretreated at 623 K was capable of adsorbing a small amount of dioxygen ($\sim 9\ \mu mol\ g^{-1}$) at 373 K. Subsequent to dioxygen adsorption, ΔH_{ads} of CO_2 on this sample was about 340 kJ mol^{-1}, which is closer to the heat of reaction for $\{Cs_2O + CO_2 \rightarrow Cs_2CO_3\}$. It is possible that bulk "Cs_2O" pretreated at 623 K partially underwent reduction to cesium suboxide. Upon dioxygen adsorption, it could have formed the stoichiometric oxide of cesium, Cs_2O.

Unlike the bulk "Cs_2O" sample, CsO_X/CsX did not adsorb dioxygen after pretreatment under vacuum at 773 K, which also supports our conclusion that the nature of the occluded species was very different from bulk "Cs_2O".

Microcalorimetry and Thermal Gravimetric Analysis of Decomposed Bulk Cesium Acetate

Since cesium acetate was the precursor used to incorporate cesium oxides in the zeolites, we proceeded to study its decomposition behavior. The heat of CO_2 adsorption at 373 K on bulk cesium acetate decomposed *in situ* under vacuum at 773 K was 134 kJ mol^{-1}. This value is significantly lower than that measured on bulk "Cs_2O" (270 kJ mol^{-1}). However, it is comparable to the initial heats of CO_2 adsorption on CsO_X/CsX and CsO_X/CsY. Infrared absorption spectroscopy on CsO_X-occluded zeolites indicated the presence of trace carbonate species, even after pretreatment in He at 773 K (18). However, bulk cesium carbonate (Aldrich, 99.995%), pretreated under vacuum at 773 K, did not adsorb any CO_2 in the microcalorimeter at 373 K. Thus, the carbonate species detected by IR spectroscopy on CsO_X/CsX are not likely to be the CO_2 adsorption sites. In an attempt to elucidate the nature of the occluded species in CsO_X/CsX, we carried out thermal decomposition of bulk cesium acetate in flowing He in a thermogravimatric analyzer (TA Instruments, TGA 2050). The weight loss of bulk cesium acetate upon heating to 773 K was 20.6%. If cesium acetate (CH_3COOCs) were to decompose to cesium carbonate (Cs_2CO_3), the weight loss would be 15.1%, whereas if it were to decompose to cesium oxide (Cs_2O), the weight loss would be 26.6%. The intermediate weight loss observed in our experiment indicates that the species formed upon cesium acetate decomposition, under our conditions, was not purely cesium carbonate or cesium oxide. Moreover, the weight loss was a function of the dioxygen concentration in the flowing gas. The weight loss decreased with increasing dioxygen concentration (20.6% in He; 16.2% in $2\%O_2/N_2$; 15.8% in air). This indicates that the nature of the species formed upon the decomposition of bulk cesium acetate was altered by the dioxygen concentration in the environment. If cesium acetate were to decompose to CsO_2 or Cs_2O_2, the weight loss would be 14.1 and 22.4%, respectively. It is likely that cesium superoxide or cesium peroxide was formed upon cesium actetate decomposition, depending on the dioxygen concentration in the flowing gas.

Effect of Sample Pretreatment and Precursor on Adsorption Properties of CsO_X/CsX

To find out if the pretreatment environment had an effect on the nature of the occluded species in CsO_X/CsX, we carried out CO_2 adsorption microcalorimetry on an uncalcined Cs(acetate)/Cs*X* sample at 373 K. The sample was pretreated *in situ* under vacuum at 773 K for 5 h prior to CO_2 adsorption. The differential heats of adsorption as a function of CO_2 uptake for this sample and the corresponding precalcined CsO_X/CsX sample were nearly identical. Although the dioxygen concentration in the pretreatment environment had an effect on the decomposition of bulk cesium acetate, it did not seem to alter the energetics of CO_2 adsorption in CsO_X/CsX.

We also investigated the effect of pretreatment temperature on the energetics of CO_2 adsorption in CsO_X/CsX. A sample pretreated at 873 K compared to 773 K showed a small increase in the energy of CO_2 adsorption ($\sim$10 kJ mol^{-1}) as well as the total CO_2 uptake ($\sim 30\ \mu mol\ g^{-1}$).

Carbon dioxide adsorption on CsO_X/CsX at 373 K was mostly reversible. The total CO_2 uptake of a CsO_X/CsX sample outgassed at 773 K for 5 h, subsequent to initial CO_2 adsorption at 373 K, was about 10% lower than that of a fresh sample. Infrared absorption spectroscopy showed that the predominant mode of CO_2 adsorption at 373 K on CsO_X-containing zeolites was the bidentate form (18).

To find out if the cesium precursor had an effect on the strengths of the base sites in CsO_X/CsX, we synthesized a CsO_X/CsX sample containing 16 occluded Cs atoms per unit cell, via incipient wetness impregnation of an aqueous solution of cesium hydroxide ($CsOH \cdot H_2O$, Aldrich). The CsOH-impregnated Cs*X* was calcined in a manner identical to the cesium acetate-impregnated Cs*X* samples described earlier. The CO_2 adsorption energies and uptakes for this sample and for CsO_X/CsX (containing 16 occluded Cs atoms per unit cell, synthesized using cesium acetate) were identical, indicating that changing the precursor from cesium acetate to cesium hydroxide did not alter the base sites in CsO_X/CsX.

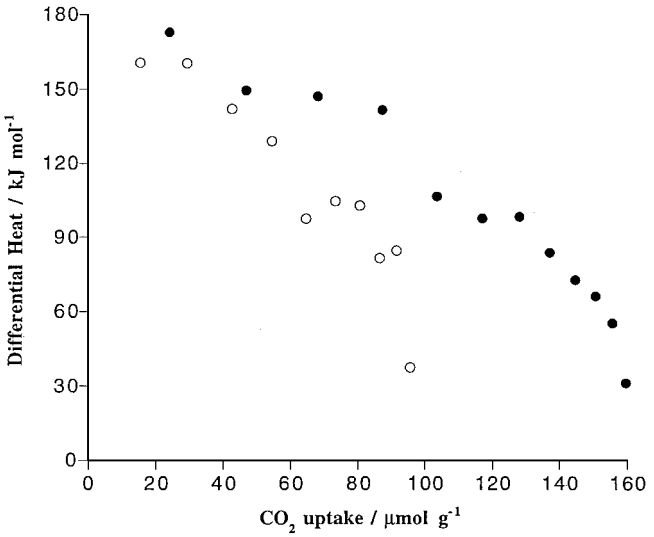

FIG. 3. Differential heats of adsorption as a function of CO_2 uptake for Cs acetate/C: (●) pretreated *in situ* under vacuum at 773 K; (○) pretreated in flowing He at 773 K and then under vacuum at 773 K.

Microcalorimetry of CO_2 Adsorption on CsO_X/Carbon

Figure 3 shows the differential heats of adsorption as a function of CO_2 uptake for CsO_X/C. The cesium acetate-modified carbon sample, pretreated *in situ* at 773 K, had a higher CO_2 uptake than a sample that was pretreated in He at 773 K and exposed to air, prior to the pretreatment for the microcalorimetry experiment. The CsO_X/C sample had the same weight loading of Cs as CsO_X/Cs*X* containing 21.3 occluded Cs atoms per unit cell. However, the total CO_2 uptake of CsO_X/C (~160 μmol g^{-1}) was significantly lower than that of CsO_X/Cs*X* (~270 μmol g^{-1}) for identical pretreatment conditions. Moreover, unlike CsO_X/Cs*X*, where the majority of the sites had uniform strength, the ΔH_{ads} values for CsO_X/C dropped rapidly with increasing coverage. Kim *et al.* showed that, for identical Cs loadings, CsO_X/C had a lower activity for 1-butene isomerization than CsO_X/Cs*X*, which led them to conclude that the nature of the occluded CsO_X species in carbon was different from that in Cs*X* (7). The authors believed that the framework oxygen atoms of the zeolite played a role in forming an active oxide of cesium. Our results from CO_2 adsorption microcalorimetry on CsO_X/C and CsO_X/Cs*X* are consistent with the observation of Kim *et al.* (7).

*Isomerization of 1-Butene on CsO_X/Cs*X**

Table 5 summarizes the reaction rates of butene isomerization over the alkali-modified catalysts at 373 K. The rate clearly increased with an increasing amount of occluded CsO_X. Figure 4 shows the rate of 1-butene isomerization normalized to the unit cell density as a function of the number of occluded Cs atoms in CsO_X/Cs*X*. A linear relationship was seen between the rate and the number of occluded Cs atoms. The turnover frequency, based on excess Cs atoms, is simply the slope of the line which is calculated to be 2×10^{-3} s^{-1}. These results are commensurate with the CO_2 adsorption capacities of these zeolites (Fig. 2). Kim *et al.* also observed an increase in the rate of 1-butene isomerization with increasing amounts of occluded cesium in Cs*X* obtained via decomposition of impregnated cesium acetate (7).

TABLE 5

Reaction Rates for the Isomerization of 1-Butene at 373 K

Catalyst[a]	No. of occluded Cs per unit cell	Rate (10^{-9} mol g^{-1} s^{-1})	2-Butene *cis*/*trans* ratio
Cs*X*	0.0	0	—
CsO_X/Cs*X*(1)	1.3	19	6.6
CsO_X/Cs*X*(2)	4.0	157	14.8
CsO_X/Cs*X*(3)	6.7	1190	19.1
CsO_X/Cs*X*(4)	10.7	988	18.8
CsO_X/Cs*X*(5)	16.0	1450	17.4
CsO_X/Cs*X*(6)	21.3	1980	19.3
Bulk "Cs_2O"	—	29	9.7
CsO_X/C (16.0 wt% Cs)	—	4	2.2

[a] Catalysts pretreated at 773 K for 2 h.

The high *cis*/*trans* ratios of the product 2-butenes (Table 5) indicate that the reaction occurred through a carbanion intermediate and hence was catalyzed by base sites. Bulk "Cs_2O" pretreated at 773 K showed lower activity per gram than the CsO_X/Cs*X* zeolites, presumably due to its low surface area. However, the *cis*/*trans* ratio for bulk "Cs_2O" was also lower than that observed for most of the CsO_X/Cs*X* zeolites. This observation supports our earlier argument

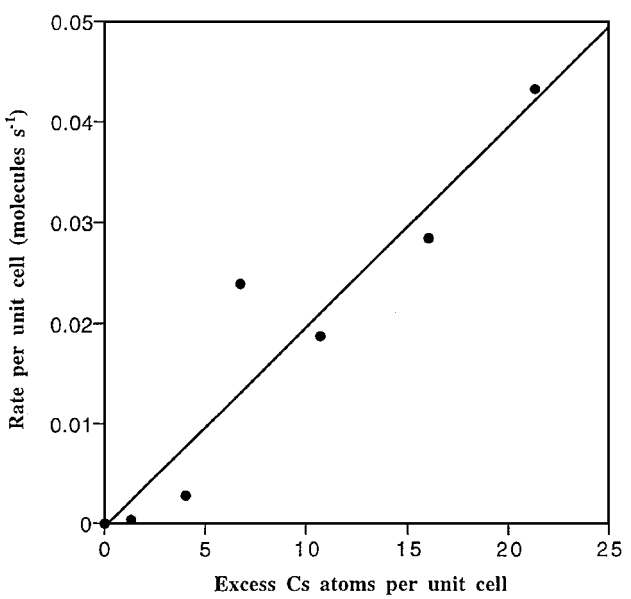

FIG. 4. Rate of 1-butene isomerization over CsO_X/Cs*X* zeolite as a function of the number of occluded Cs atoms.

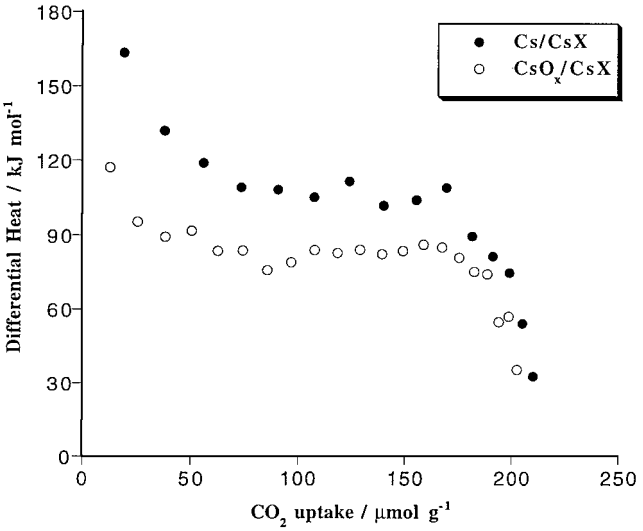

FIG. 5. Differential heats of adsorption as a function of CO_2 uptake for Cs/Cs*X* (20 occluded Cs atoms per unit cell) and CsO_X/Cs*X* (16 occluded Cs atoms per unit cell).

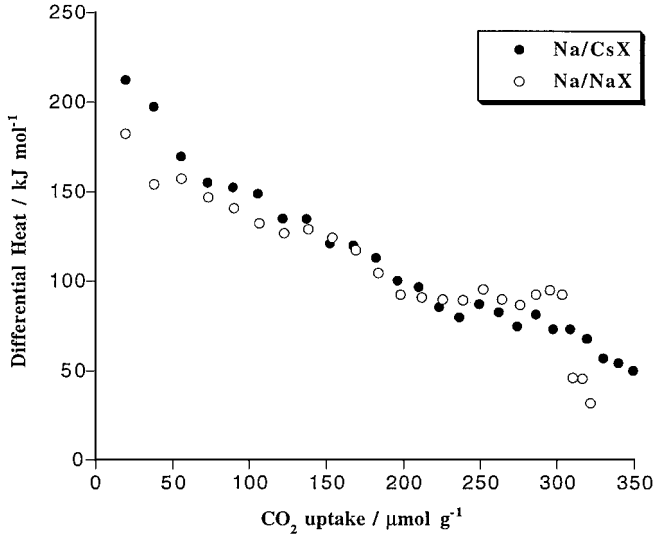

FIG. 6. Differential heats of adsorption as a function of CO_2 uptake for Na/Na*X* and Na/Cs*X*.

that the nature of the occluded Cs species in CsO_X/Cs*X* is different from a bulk "Cs_2O" supplied by Aldrich. The CsO_X/C catalyst also showed a lower activity and *cis*/*trans* ratio for the reaction compared to the CsO_X/Cs*X* zeolites. This indicates that the nature of the occluded CsO_X species in CsO_X/C is different from that of CsO_X/Cs*X*. Our results from CO_2 adsorption microcalorimetry also support this conclusion.

Microcalorimetry of CO_2 Adsorption on Zeolites Containing Occluded Alkali Metals

Figure 5 shows the differential heats of adsorption as a function of CO_2 uptake for Cs/Cs*X*. The thermogram for CsO_X/Cs*X* is included for comparison. The majority of the CO_2 adsorption sites in Cs/Cs*X* were about 30 kJ mol^{-1} higher in energy than those in CsO_X/Cs*X*. Figure 6 shows ΔH_{ads} of CO_2 as a function of surface coverage for Na/Na*X* and Na/Cs*X*. Apparently, changing the exchange cation from Na to Cs did not affect the strengths of CO_2 adsorption on Na occluded in *X* zeolite. The ratio of the number of CO_2 molecules adsorbed to the number of occluded Na atoms in Na/Na*X* and Na/Cs*X* was about 1 : 10. Perhaps a part of the occluded Na was located in the sodalite cages of the zeolite and was inaccessible to CO_2. It is also possible that the occluded Na clusters were sufficiently large to prevent CO_2 interaction with each occluded Na atom.

Figure 7 shows ΔH_{ads} versus surface coverage for CO_2 adsorption on Cs/Na*X* and Cs/Na*Y*. Cs/Na*Y* had fewer CO_2 adsorption sites than Cs/Na*X*. Similarly, Na/Na*Y* (Fig. 8) had fewer CO_2 adsorption sites than Na/Na*X* (Fig. 6). We suspect that the higher Si content of the *Y* zeolite allowed for the formation of weakly basic alkali metal silicates by partial destruction of the framework. To assess the reversibility of CO_2 adsorption on the occluded alkali metal in zeolite, the Na/Na*Y* sample was evacuated at 773 K for 5 h after CO_2 adsorption, and then CO_2 was adsorbed again on the sample at 373 K. Figure 8 shows that CO_2 adsorption on Na/Na*Y* was mostly irreversible. Paul *et al.* studied CO_2 adsorption and decomposition on bulk polycrystalline alkali metals using electron energy loss spectroscopy (EELS) and thermal desorption (24). The authors suggested three possible reaction paths for CO_2 adsorbed on bulk alkali metals at 100 K. The first path involved reversible weak adsorption of molecular CO_2. The second path involved instantaneous oxygen abstraction from CO_2 by the alkali metal, leading to the formation of CO. The third path involved the

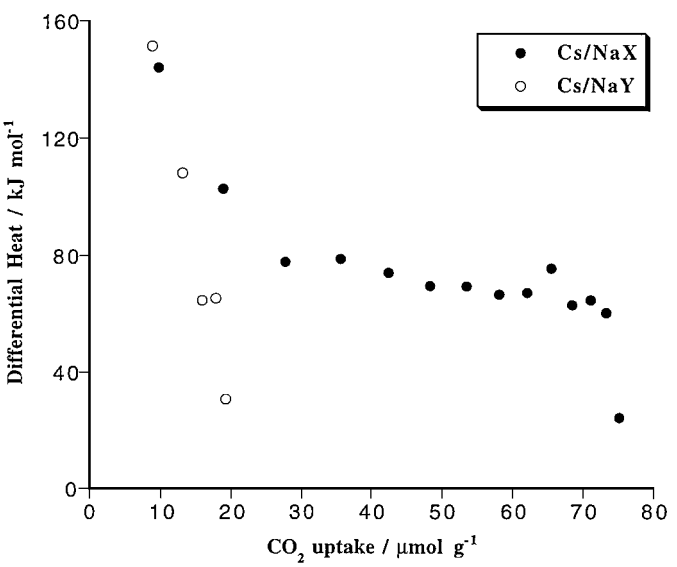

FIG. 7. Differential heats of adsorption as a function of CO_2 uptake for Cs/Na*X* and Cs/Na*Y*.

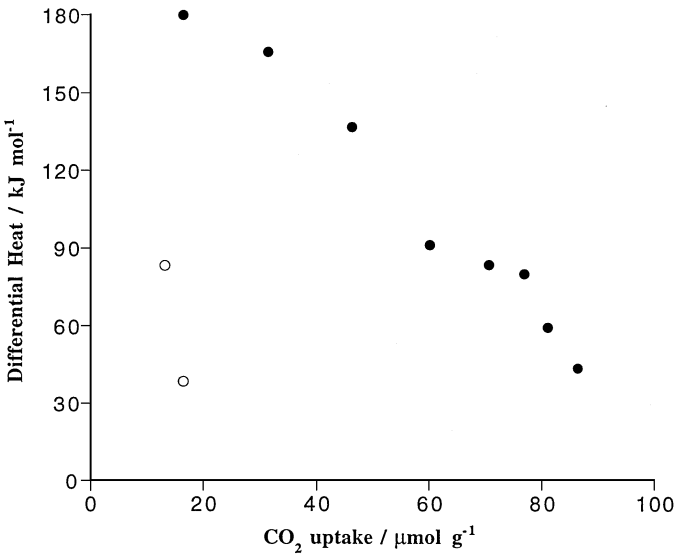

FIG. 8. Differential heats of adsorption as a function of CO_2 uptake for Na/NaY: (●) CO_2 adsorption at 373 K; (○) sample was outgassed at 773 K after initial CO_2 adsorption, and then CO_2 was adsorbed again at 373 K.

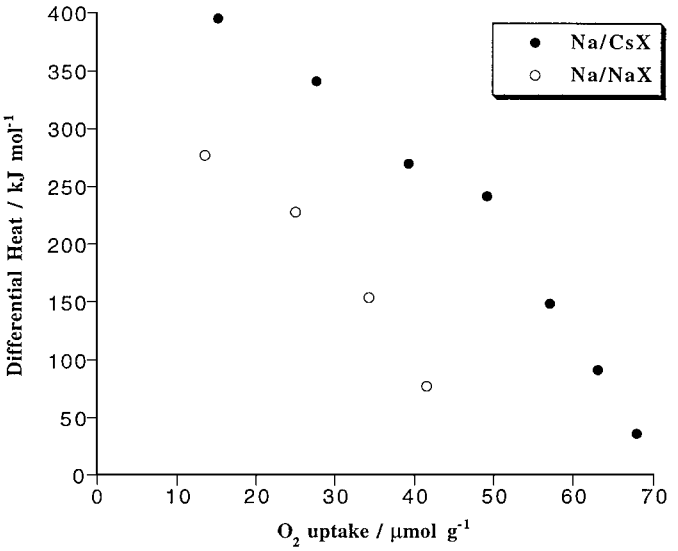

FIG. 9. Differential heats of adsorption as a function of O_2 uptake for Na/Cs*X* and Na/Na*X*.

formation of CO_2^- due to electron transfer at the surface, dimerization of CO_2^- to oxalate ($C_2O_4^-$), decomposition of the oxalate into CO_3^{2-} and CO, and finally decomposition of the alkali metal carbonate at 540 K to CO_2, alkali metal atoms/ions, and O_2^- ions. Since CO_2 adsorption on our alkali metal/zeolite samples was not reversible (Fig. 8), the adsorbed CO_2 possibly underwent decomposition upon heating the sample to 773 K, resulting in poisoning of the alkali metal.

Microcalorimetry of O_2 Adsorption on Zeolites Containing Occluded Alkali Metals

Since the decomposition of alkali azides impregnated in zeolites created alkali metal clusters, dioxygen adsorption on these clusters should result in the formation of alkali oxides. To probe the effect of dioxygen adsorption on the basicity of alkali metal-occluded zeolites, we carried out dioxygen adsorption experiments on these zeolites in the microcalorimeter at 373 K. The zeolites were pretreated *in situ* using the same pretreatment procedure described earlier. Figure 9 shows the differential heats of adsorption as a function of O_2 uptake for Na/Cs*X* and Na/Na*X*. The initial heat of O_2 adsorption on Na/Cs*X* was about 400 kJ mol^{-1}. The color of this sample after O_2 adsorption was pale yellow, which possibly indicates the formation of Na_2O_2. Also, the O_2 adsorption on these samples was irreversible. Barrer *et al.* also proposed the formation of Na_2O_2 during the decomposition of intracrystalline NaN_3 in cancrinite due to the reaction of dioxygen with the azide itself or with the Na metal generated from the azide decomposition (25). As seen in Fig. 9, the initial ΔH_{ads} and the total O_2 uptake for Na/Na*X* was lower than those for Na/Cs*X*. The lower O_2 adsorption capacity of Na/Na*X* was likely due to its lower loading of occluded alkali metal.

After O_2 adsorption on Na/Na*X* and Na/Cs*X*, the samples were outgassed overnight at 373 K and then CO_2 adsorption was carried out at 373 K. Figure 10 shows the ΔH_{ads} as a function of CO_2 uptake for these samples, subsequent to dioxygen adsorption. A comparison of Figs. 10 and 6 shows that the CO_2 uptakes of these samples decreased significantly, subsequent to O_2 adsorption. Thus, O_2 adsorption on Na/Na*X* and Na/Cs*X* resulted in poisoning of some of the CO_2 adsorption sites in these zeolites. Table 6 shows the O_2 uptakes of the alkali metal-containing zeolites and their

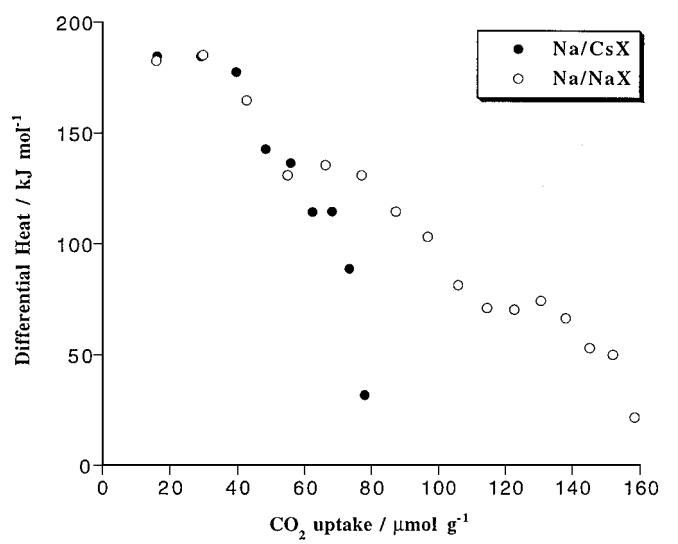

FIG. 10. Differential heats of adsorption as a function of CO_2 uptake for Na/Cs*X* and Na/Na*X* after O_2 adsorption.

TABLE 6

CO_2 and O_2 Adsorption Capacities of Alkali Metal-Occluded Zeolites

Zeolite	Occluded alkali (μmol/g)	CO_2 adsorption capacity (μmol/g)	O_2 adsorption capacity (μmol/g)	CO_2 uptake after O_2 adsorption (μmol/g)	ΔCO_2 per O_2 adsorbed[a]
Na/Cs*X*	3078	349	68	78	3.99
Na/Na*X*	3078	322	42	158	3.90
Cs/Cs*X*	943	210	11	164	4.18
Cs/Na*X*	545	75	3	67	2.67
Na/Na*Y*	3078	86	7	65	3.00
Cs/Na*Y*	943	19	3	21	—

[a] Decrease in CO_2 adsorption capacity divided by the O_2 adsorption capacity.

CO_2 adsorption capacities before and after O_2 adsorption. The CO_2 adsorption capacity of all the alkali metal-containing zeolites decreased after O_2 adsorption. Interestingly, the difference in CO_2 uptakes before and after O_2 adsorption was about 4 times the amount of O_2 adsorbed (Table 6). Therefore, assuming dissociative adsorption of O_2, one oxygen atom poisons about two CO_2 adsorption sites. The CO_2 and O_2 adsorption capacities of these zeolites were low compared to the amount of occluded alkali present in them.

We also tested for the reversibility of CO_2 adsorption after O_2 adsorption on Na/Na*X* by outgassing the sample at 773 K for 5 h and then adsorbing CO_2 on the sample again. Figure 11 shows that the CO_2 adsorption on Na/Na*X* after O_2 adsorption was not completely reversible. At this point, we are unable to say whether the CO_2 adsorption after O_2 adsorption on the alkali metal-containing zeolites is occurring over the "alkali oxide" or the unreacted alkali metal.

Surface Analysis by X-ray Photoelectron Spectroscopy

Analysis by XPS provided insights into the distribution of alkali species on the zeolite samples. The Cs/Si ratios for Cs*X*, CsO_X/Cs*X* (16 occluded Cs atoms/unit cell) and Cs/Cs*X* obtained from XPS analysis, ranged from 0.43 to 0.46, indicating negligible surface enrichment of Cs for CsO_X/Cs*X* and Cs/Cs*X*. For comparison, the Cs/Si ratio for Cs*X* obtained from bulk elemental analysis was 0.36. Thus, the "CsO_X" and Cs metal species seemed to be well-occluded in the zeolite cages. However, the Cs*X* zeolite impregnated with NaN_3 showed interesting results. Before decomposition of the impregnated azide, the Na/Si ratio in this sample was 0.56, which is lower than that in the bulk (~1.0). This indicates that most of the impregnated NaN_3 was located in the cages of Cs*X*. However, after azide decomposition, the surface Na/Si ratio was 1.63, which is greater than the bulk ratio. Apparently, some of the Na metal species migrated to the surface upon decomposition of NaN_3. This was not observed in the case of CsN_3-containing Cs*X* within the sensitivity of the XPS technique. However, the loading of NaN_3 in Cs*X* (67 Na atoms per unit cell) was much higher than the CsN_3 loading in Cs*X* (20 Cs atoms per unit cell), which could have facilitated the migration of Na out of the zeolite cages on to the external surface upon heating.

Microcalorimetry of CO_2 and O_2 Adsorption on Na/Carbon

Figure 12 shows the differential heats of CO_2 adsorption as a function of surface coverage for Na/C. Unlike

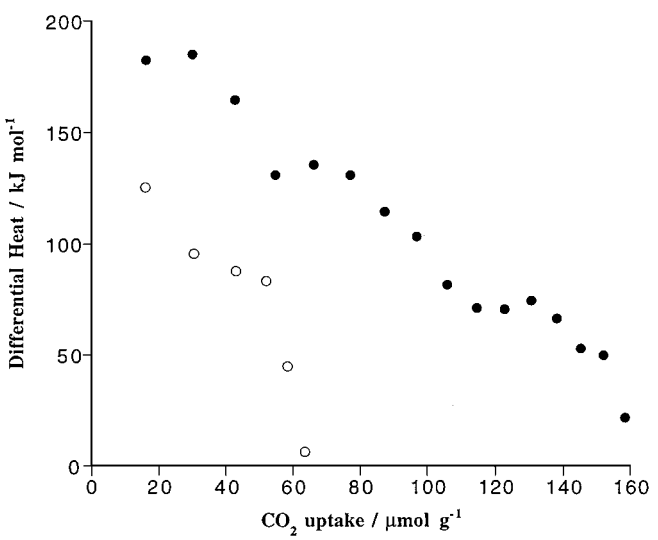

FIG. 11. Differential heats of adsorption as a function of CO_2 uptake after O_2 adsorption on Na/Na*X*: (●) CO_2 adsorption at 373 K; (○) sample was outgassed at 773 K after initial CO_2 adsorption, and then CO_2 was adsorbed again at 373 K.

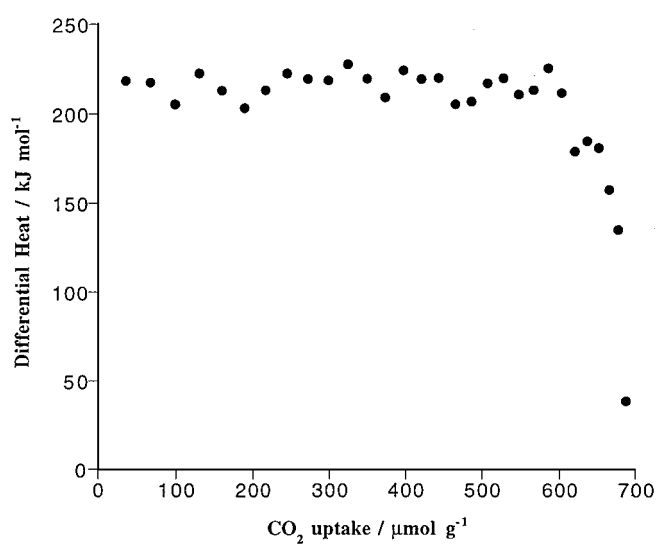

FIG. 12. Differential heats of adsorption as a function of CO_2 uptake for Na/C.

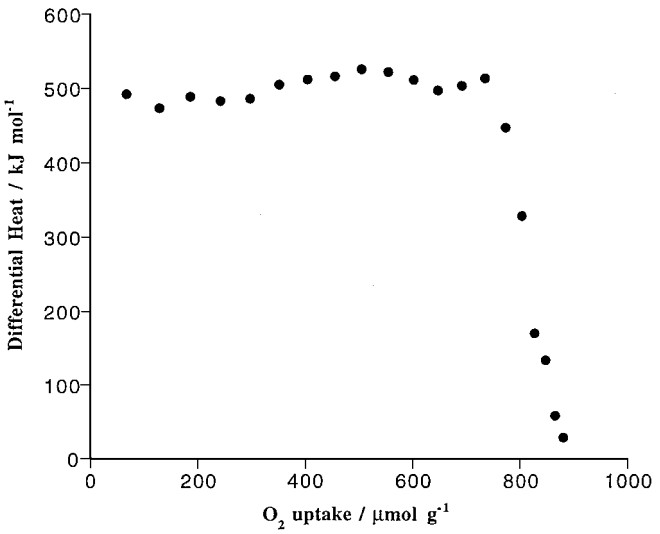

FIG. 13. Differential heats of adsorption as a function of O_2 uptake for Na/C.

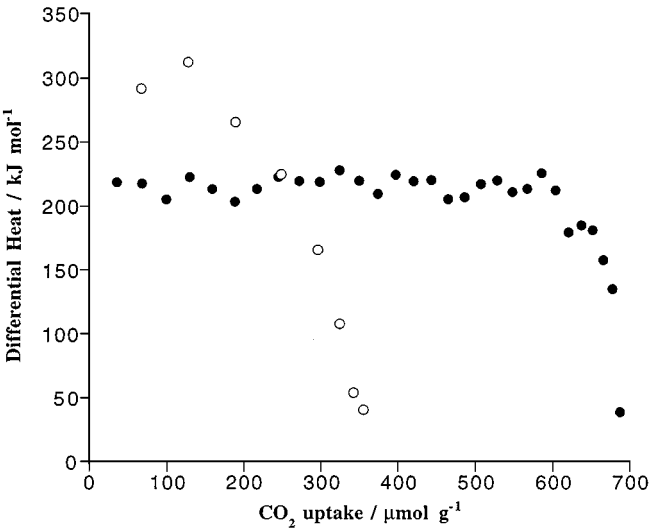

FIG. 14. Differential heats of adsorption as a function of CO_2 uptake for Na/C: (●) before O_2 adsorption; (○) after O_2 adsorption.

Na metal occluded in zeolites, where the ΔH_{ads} decreased with increasing CO_2 uptake (Fig. 6), the majority of the sites in Na/C had similar CO_2 adsorption energies (~220 kJ mol^{-1}). Also, the total CO_2 uptake for Na/C was higher than that for Na/Na*X* or Na/Cs*X*, for the same weight loading of occluded Na. Similar to the case of CO_2 adsorption, the O_2 adsorption energies for the majority of the sites in Na/C were uniform (Fig. 13). Dioxygen adsorption on the bare carbon support was insignificant (~5 μmol g^{-1}) in comparison to that on Na/C (~880 μmol g^{-1}). Dioxygen adsorption on Na/C possibly led to the formation of surface peroxide, Na_2O_2. The theoretical heat of reaction for $\{2Na + O_2 \rightarrow Na_2O_2\}$, obtained from heats of formation, was −511 kJ mol^{-1} (23). Considering the heats of formation of NaO_2 and Na_2O from Na and O_2 are −260 and −414 kJ mol^{-1}, respectively (23), the heats evolved per mole of O_2 adsorbed, in the formation of NaO_2, Na_2O_2, and Na_2O from Na and O_2, would be 260, 511, and 828 kJ, respectively. The measured heat of O_2 adsorption on Na/C shown in Fig. 13 (~500 kJ mol^{-1}) agrees well with the formation of Na_2O_2. Similar to the results on alkali metals occluded in the zeolites, dioxygen adsorption resulted in the poisoning of some of the CO_2 adsorption sites in Na/C (Fig. 14). The high initial heats of CO_2 adsorption (around 300 kJ mol^{-1}) for Na/C exposed to O_2 (Fig. 14) may result from CO_2 adsorption on Na_2O_2. For similar loadings of occluded Na in zeolites and carbon, the carbon sample exhibited higher CO_2 and O_2 uptakes. Perhaps the carbon support provided a better dispersion of alkali metal atoms on the surface. Since the uniformity of the CO_2 and O_2 adsorption sites on Na/C was not observed for the alkali metal-loaded zeolites, we speculate that the alkali metals strongly interact, or react, with the zeolite framework.

Isomerization of 1-Butene on Zeolites Containing Occluded Alkali Metals

A sample with cesium metal occluded in Cs*X* (Cs/Cs*X*) showed comparable activity for 1-butene isomerization (Table 7) as similarly loaded CsO_X/Cs*X* (Table 5). To investigate the effect of O_2 poisoning on the activity of Cs/Cs*X* for 1-butene isomerization, dioxygen was adsorbed at 373 K on Cs/Cs*X* after pretreatment at 873 K. The sample was then purged with He for 0.5 h prior to the reaction. Dioxygen adsorption at 373 K resulted in an order of magnitude decrease in the activity of Cs/Cs*X* (Table 7). However, when Cs/Cs*X* was heated at 773 K for 1.5 h after O_2 adsorption at 373 K, the activity was almost fully recovered. On the basis of the results from microcalorimetry, dioxygen adsorption on Cs/Cs*X* was irreversible after it was heated to 773 K. Hence, heating Cs/Cs*X* to 773 K after O_2 adsorption must result in the formation of an active alkali oxide species. At this point, the stoichiometry of this oxide is unclear. Yagi *et al.* reported a similar trend for CsO_X/Cs*X* (21). Upon O_2

TABLE 7

Isomerization of 1-Butene over Cs/Cs*X* at 373 K

Catalyst	No. of occluded Cs per unit cell	Rate (10^{-9} mol g^{-1} s^{-1})	2-Butene *cis*/*trans* ratio
Cs/Cs*X*[a]	20.0	1630	12.0
Cs/Cs*X*[b]	20.0	282	13.9
Cs/Cs*X*[c]	20.0	1590	11.1

[a] Pretreated at 873 K for 5 h.
[b] Pretreated at 873 K for 5 h and then O_2 adsorbed at 373 K.
[c] Pretreated at 873 K for 5 h and then O_2 adsorbed at 373 K, after which the sample was heated at 773 K for 1.5 h.

TABLE 8

Reaction Rates for the Alkylation of Toluene with Ethylene at 523 K

Catalyst	Rate[a] (10^{-9} mol g^{-1} s^{-1})	Conversion (%)	% Selectivity to side-chain alkylates		
			mono	di	tri
Na/Na*X*	305	11.8	68.4	31.6	0.0
Na/Na*X*[b]	47	1.8	83.7	16.3	0.0
Na/Cs*X*	407	15.8	75.6	21.8	2.6
Cs/Na*X*	5	0.4	100	0.0	0.0
Cs/Cs*X*	268	10.2	75.3	20.2	4.5
Cs/Cs*X*[b]	29	1.1	100	0.0	0.0
Na/C	12	0.5	100	0.0	0.0

[a] Rate based on toluene conversion reported after 15 min on stream.
[b] O_2 adsorbed at room temperature prior to the reaction.

adsorption on CsO_X/Cs*X*, the authors found that the activity for 1-butene isomerization was eliminated. However, when the catalyst was heated to 673 K after O_2 adsorption, the activity was recovered (23).

Alkylation of Toluene with Ethylene over Catalysts Containing Occluded Alkali Metals

Since exploratory tests with catalysts containing CsO_X did not reveal any products of the toluene alkylation reaction by GC analysis, we focused on the zeolites containing alkali metal. The activities of these metal-containing samples for the alkylation of toluene with ethylene at 523 K are reported in Table 8. The rates and conversions were based on toluene since ethylene was present in great excess. Side-chain alkylates were the only products detected by gas chromatography. The activities of Na/Na*X*, Na/Cs*X*, and Cs/Cs*X* for the alkylation reaction were higher than those of Cs/Na*X*. However, Cs/Na*X* had a smaller number of occluded alkali atoms and a lower CO_2 adsorption capacity than either Na/Na*X* or Na/Cs*X*, which is consistent with the lower activity of this catalyst for the alkylation reaction. The alkali metals occluded in *Y* zeolites (Na/Na*Y* and Cs/Na*Y*) showed no activity for the reaction under our conditions. The CO_2 adsorption capacities of Na/Na*Y* (Fig. 8) and Cs/Na*Y* (Fig. 7) were also lower than those of the analogous *X* zeolites. Martens *et al.* saw a higher activity for a Na metal-containing Na*X* zeolite compared to that of the corresponding *Y* zeolite in the ethylation of toluene at 523 K (26). Our Na/C catalyst exhibited very little activity for the alkylation reaction. Strangely, the CO_2 uptake on Na/C (Fig. 12) was higher than the Na metal-containing *X* zeolites (Fig. 6) and the majority of the CO_2 adsorption sites in Na/C had strengths higher than 200 kJ mol^{-1}. One possible explanation is that the Na metal atoms located in the micropores of carbon were accessible to a small molecule like CO_2, but inaccessible to toluene. It is also possible that the zeolite plays a role in stabilizing adsorbed toluene. It was proposed that the alkali cations in the zeolite framework can stabilize aromatics by interacting with the π-electron cloud of the aromatic ring (2, 27). Although CsO_X/Cs*X* and CsO_X/C pretreated at 773 K were active for the isomerization of 1-butene, these catalysts were inactive for toluene ethylation at 523 K. The alkylation reaction was apparently more demanding and occurred only over occluded alkali metals. The number of turnovers after about 2 h on stream, based on O_2 adsorption capacity (Table 9), indicated that the alkylation reaction was catalytic and not stoichiometric.

It has been proposed that side-chain alkylation of toluene with olefins over base catalysts occurs through a carbanion mechanism (26). Pines and Mark studied the side-chain alkylation of aromatics with mono-olefins in the presence of Na metal in organic solvents (28). They found that isobutylbenzene was the predominant product formed in the alkylation of toluene with propene. Since the order of carbanion stability is primary > secondary > tertiary, which is opposite to that of carbonium ions and free radicals, the authors concluded that the alkylation reaction was occurring via a carbanion intermediate. We also carried out the alkylation of toluene with propene over Na/Na*X* at 523 K and observed that isobutylbenzene was the only product formed. This is consistent with the observation of Pines and Mark (28) and suggests a carbanion mechanism for the alkylation reaction.

Table 8 also shows the activity of Na/Na*X* and Cs/Cs*X* for toluene alkylation with ethylene subsequent to dioxygen adsorption. After catalyst pretreatment, O_2 was adsorbed at room temperature and the catalyst was heated to the reaction temperature in flowing He. As seen in Table 8, O_2 adsorption on Na/Na*X* and Cs/Cs*X* resulted in an order of magnitude decrease in activity for the alkylation reaction. A similar result was obtained on Cs/Cs*X* for the isomerization of 1-butene (Table 7). However, Cs/Cs*X* was heated to 773 K after O_2 adsorption, the catalyst recovered its activity for 1-butene isomerization, whereas a similar treatment completely eliminated the activity for the

TABLE 9

Number of Turnovers for the Alkylation of Toluene with Ethylene at 523 K

Catalyst	No. of turnovers based on no. of occluded alkali atoms	No. of turnovers based on CO_2 adsorption capacity	No. of turnovers based on O_2 adsorption capacity
Na/Na*X*	0.33	3.20	24.5
Na/Cs*X*	0.50	4.44	22.8
Cs/Na*X*	0.03	0.24	5.9
Cs/Cs*X*	0.42	1.87	35.6
Na/C	0.09	0.40	0.31

Note. After approximately 2 h on stream.

alkylation reaction. Perhaps O_2 adsorption at lower temperatures converted only a part of the occluded alkali metal species into an alkali oxide, leaving some alkali metal species. Upon the O_2-poisoned catalyst being heated to 773 K, all of the reactive alkali metal might have converted into an alkali oxide. This heated, oxygen-poisoned catalyst was active for the isomerization of 1-butene but showed no reactivity for the alkylation of toluene with ethylene.

CONCLUSIONS

The energetics of the base sites in alkali-modified zeolites were obtained using adsorption microcalorimetry of carbon dioxide. Zeolites containing occluded CsO_X clusters had higher CO_2 adsorption capacities and heats of adsorption compared to the alkali-exchanged zeolites. The majority of the base sites in the alkali oxide-containing zeolites had uniform strength. The number of CO_2 adsorption sites in zeolites containing occluded CsO_X was directly proportional to the amount of occluded cesium, with one CO_2 molecule being adsorbed for every four occluded Cs atoms. Our measured heats of CO_2 adsorption on zeolites containing CsO_X are significantly lower than the measured heat of adsorption on a bulk cesium oxide and the heat of reaction of Cs_2O and CO_2 to form Cs_2CO_3. These results, together with our observed CO_2 adsorption stoichiometry, suggest that the intrazeolitic CsO_X clusters are not simply Cs_2O. The activity of CsO_X-containing zeolites for 1-butene isomerization increased linearly with the amount of occluded cesium, which is consistent with the trend of CO_2 adsorption capacities.

The CsO_X-containing microporous carbon was less active for 1-butene isomerization, indicating that the alkali oxide on the carbon support is quite different in nature from that on the zeolite support.

Alkali metal-containing zeolites were found to have stronger CO_2 adsorption sites than alkali oxide-containing zeolites. Dioxygen adsorption on zeolites containing occluded alkali metals led to poisoning of some of the CO_2 adsorption sites with a stoichiometry of one oxygen atom per two CO_2 adsorption sites. Comparison of the CO_2 and O_2 adsorption thermograms for the alkali metal-loaded zeolites and carbon suggests that the alkali metals interact strongly with the zeolite framework. Zeolites containing occluded alkali metals were active for the side-chain alkylation of toluene with ethylene, whereas zeolites containing occluded alkali oxides were inactive for the reaction. Dioxygen adsorption on alkali metal occluded in zeolites resulted in reduced catalytic activity of these materials for 1-butene isomerization and toluene alkylation. However, heating these catalysts to 773 K after dioxygen adsorption resulted in recovery of their activity for 1-butene isomerization, but completely eliminated their activity for toluene alkylation. Apparently, all of the active alkali metal is transformed into an alkali oxide after O_2 adsorption and heating to a high temperature. Although the alkali oxide thus formed is active for 1-butene isomerization, it is inactive for the more demanding alkylation reaction.

ACKNOWLEDGMENTS

This work was supported by the Department of Energy (Basic Energy Sciences, Grant DEFG05-95ER14549).

REFERENCES

1. Tsuji, H., Yagi, F., Hattori, H., and Kita, H., *Stud. Surf. Sci. Catal.* **75**, 1171 (1993).
2. Barthomeuf, D., *Catal. Rev.-Sci. Eng.* **38**, 521 (1996).
3. Hathaway, P. E., and Davis, M. E., *J. Catal.* **116**, 263 (1989).
4. Corma, A., Fornes, V., Martin-Aranda, R. M., Garcia, H., and Primo, J., *Appl. Catal.* **59**, 237 (1990).
5. Wieland, W. S., Davis, R. J., and Garces, J. M., *J. Catal.* **173**, 490 (1998).
6. Lasperas, M., Cambon, H., Brunel, D., Rodriguez, I., and Geneste, P., *Micro. Mater.* **7**, 61 (1996).
7. Kim, J. C., Li, H. X., Chen, C. Y., and Davis, M. E., *Micro. Mater.* **2**, 413 (1994).
8. Rodriguez, I., Cambon, H., Brunel, D., Lasperas, M., and Geneste, P., *Stud. Surf. Sci. Catal.* **78**, 623 (1993).
9. Rodriguez, I., Cambon, H., Brunel, D., and Lasperas, M., *J. Mol. Catal. A: Chem.* **130**, 195 (1998).
10. Harrison, M. R., Edwards, P. P., Klinowski, J., and Thomas, J. M., *J. Solid State Chem.* **54**, 330 (1984).
11. Martens, L. R. M., Grobet, P. J., Vermeiren, W. J. M., and Jacobs, P. A., *Stud. Surf. Sci. Catal.* **28**, 935 (1986).
12. Martens, L. R. M., Vermeiren, W. J. M., Grobet, P. J., and Jacobs, P. A., *Stud. Surf. Sci. Catal.* **31**, 531 (1987).
13. Xu, B., and Kevan, L., *J. Chem. Soc., Faraday Trans.* **88**, 1695 (1992).
14. Xu, B., and Kevan, L., *J. Phys. Chem.* **96**, 2642 (1992).
15. Sun, T., Seff, K., Heo, N. H., and Petranovskii, V. P., *J. Phys. Chem.* **98**, 5768 (1994).
16. Pines, H., and Stalik, W. M., "Base-Catalyzed Reactions of Hydrocarbons and Related Compounds." Academic Press, New York, 1977.
17. Martens, L. R. M., Grobet, P. J., and Jacobs, P. A., *Nature* **315**, 568 (1985).
18. Doskocil, E. J., and Davis R. J., *J. Catal.*, in press.
19. Bordawekar, S. V., Doskocil, E. J., and Davis, R. J., *Langmuir* **14**, 1734 (1998).
20. Hathaway, P. E., and Davis, M. E., *J. Catal.* **116**, 279 (1989).
21. Yagi, F., and Hattori, H., *Micro. Mater.* **9**, 247 (1997).
22. Krawietz, T. R., Murray, D. K., and Haw, J. F., *J. Phys. Chem. A* **102**, 8779 (1998).
23. Lide, D. R., Ed. "CRC Handbook of Chemistry and Physics," 71st ed. CRC Press, Boca Raton, FL, 1990.
24. Paul, J., Hoffmann, F. M., and Robbins, J. L., *J. Phys. Chem.* **92**, 6967 (1988).
25. Barrer, R. M., Daniels, E. A., and Madigan, G. A., *J. Chem. Soc., Dalton Trans.* 1805 (1976).
26. Martens, L. R., Vermeiren, W. J., Huybrechts, D. R., Grobet, P. J., and Jacobs, P. A., "Proceedings, 9th International Congress on Catalysis, Calgary, 1988" (M. J. Phillips and M. Ternan, Eds.), p. 420. Chem. Institute of Canada, Ottawa, 1988.
27. Palomares, A. E., Eder-Mirth, G., Rep, M., and Lercher, J. A., *J. Catal.* **180**, 56 (1998).
28. Pines, H., and Mark, V., *J. Am. Chem. Soc.* **78**, 4316 (1956).